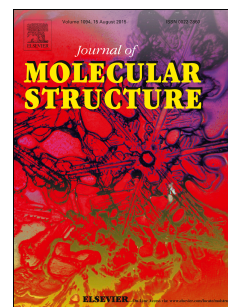


Accepted Manuscript

Study of structural and catalytic properties of Ni catalysts prepared from inorganic complex precursor for Fischer-Tropsch synthesis

Sania Saheli, Ali Reza Rezvani, Azim Malekzadeh



PII: S0022-2860(17)30610-5

DOI: [10.1016/j.molstruc.2017.05.027](https://doi.org/10.1016/j.molstruc.2017.05.027)

Reference: MOLSTR 23768

To appear in: *Journal of Molecular Structure*

Received Date: 10 December 2016

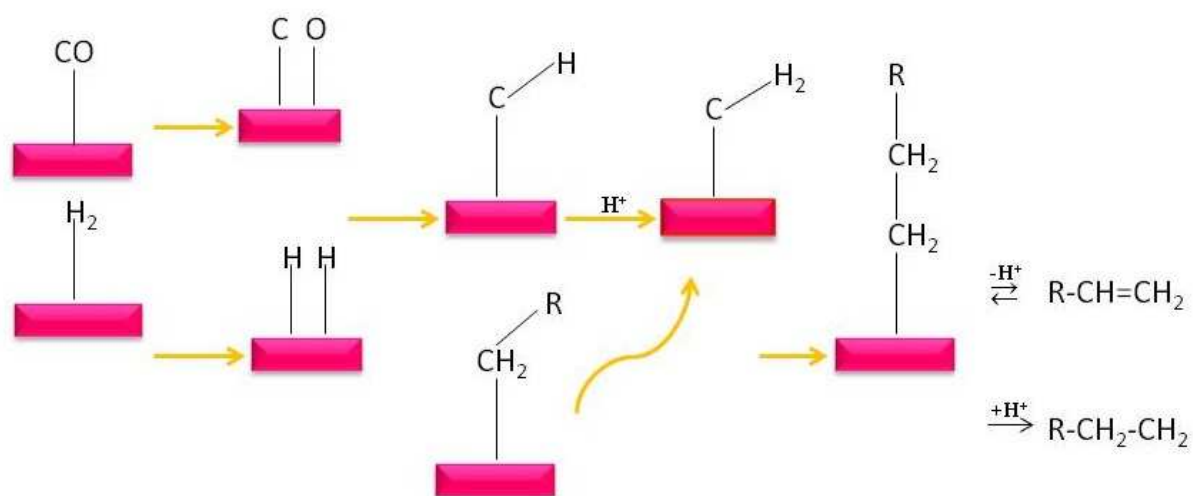
Revised Date: 25 April 2017

Accepted Date: 10 May 2017

Please cite this article as: S. Saheli, A.R. Rezvani, A. Malekzadeh, Study of structural and catalytic properties of Ni catalysts prepared from inorganic complex precursor for Fischer-Tropsch synthesis, *Journal of Molecular Structure* (2017), doi: 10.1016/j.molstruc.2017.05.027.

This is a PDF file of an unedited manuscript that has been accepted for publication. As a service to our customers we are providing this early version of the manuscript. The manuscript will undergo copyediting, typesetting, and review of the resulting proof before it is published in its final form. Please note that during the production process errors may be discovered which could affect the content, and all legal disclaimers that apply to the journal pertain.

Graphical abstract



Study of structural and catalytic properties of Ni catalysts prepared from inorganic complex precursor for Fischer-Tropsch synthesis

Sania Saheli ^a, Ali Reza Rezvani ^{a,*}, Azim Malekzadeh ^b

^a Department of Chemistry, University of Sistan and Baluchestan, P. O. Box 98135-674, Zahedan, Iran

^b School of Chemistry, Damghan University (DU), Damghan, Iran

*E-mail address: Ali@hamoon.usb.ac.ir

Abstract

The silica- and alumina- supported Ni catalysts synthesized by thermal decomposition of inorganic precursors were evaluated for Fischer–Tropsch synthesis (FTS); the structural properties and performance of the catalysts were compared to those of samples constructed via impregnation method. The results revealed that the synthesized catalysts have higher catalytic activity comparison to those prepared via the conventional impregnation method. The effect of the preparation method on the structural properties shows that synthesizing the catalyst through inorganic precursor route is more appropriate. Characterization of catalysts is carried out using inductively coupled plasma (ICP), powder X-ray diffraction (XRD), scanning electron microscopy (SEM), and BET specific surface area.

Keywords: Coordination polymers; Inorganic precursor; Impregnation; Fischer-Tropsch synthesis; Nickel catalyst; Synthesis route.

1. Introduction

In recent years, the Fischer–Tropsch synthesis (FTS) has received considerable attention from academic institutions and governments alike, due to environmental contamination, rapidly rising price of crude oil and subtractive oil reserves [1–3]. The FTS is a viable route for the production of clean fuels from biomass-derived syngas, natural gas, or coal. In this process, highly important factor is a catalyst, which is selected based on the key role in product distribution [4, 5].

Group VIII transition metals are highly able to catalyze the FTS. This performance for FTS is defined by the nature of CO and H₂ adsorption on the group VIII transition metals [6]; moreover, these metals demonstrate some acting in the C–C coupling reaction during hydrogenation of

carbon monoxide. Among the group VIII transition metals which are catalyzed the FTS; the more active metals are iron, cobalt, nickel and ruthenium [7–10]. However, iron and cobalt are rather considered due to selectivity and cost [11]. In the FTS, nickel used less owing to methane selectivity while in many of the catalytic researches, based on iron or cobalt catalysts, nickel has improved the catalyst performance [12, 13]. In recent study carried out by Enger et al. [14], it was shown that the Ni might be capable to generate different productions and methane in not only product of FTS. Moreover, some factors such as support, CO/H₂ ratio and particles size of catalyst can affect to FTS productions. Apart from these factors, production procedure of the catalyst strongly affects the outcomes of FTS. Most of the catalysts for FTS manufactured by co-precipitation, sol-gel, impregnation and fusion methods [15–20] while use of the inorganic precursor complexes as novel technique for preparing materials create some benefit such as lower particle sizes and the homogeneous dispersion of metals on the support surface which increase catalyst performance [21].

To date, coordination polymers or metal–organic frameworks showing various novel structures and intriguing properties in the field of catalyst [22–24], however, the role of these types of combinations as catalyst precursor for FTS have not been explored. Recently, through the self-assembly reaction of H₃btc and Ni(NO₃)₂, we have successfully isolated a new coordination polymer with interesting geometry, [Ni(H₂btc)(OH)(H₂O)₂] [25]. Considering the importance of FTS and the unique ability of metal–Organic frameworks to create special topology, in this work, the inorganic precursors [Ni(H₂btc)(OH)(H₂O)₂]/SiO₂ and [Ni(H₂btc)(OH)(H₂O)₂]/Al₂O₃ are used to prepare Ni catalysts, furthermore, evaluated the catalytic performance of these catalysts and compared with reference catalysts which are produced by impregnation method. Also, respective studies on the physicochemical characteristics performed by X-ray diffraction, Brunauer-Emmett-Teller and scanning electron microscope.

2. Experimental

2.1. Materials

All the used chemicals were reagent grade and used without further purification, purchased from Aldrich.

2.2. Synthesis of complex

$\text{Ni}(\text{NO}_3)_2 \cdot 6\text{H}_2\text{O}$ (0.290 g , 1.0 mmol), 1,3,5-benzenetricarboxylic acid (0.105 g , 0.5 mmol), NaOH (0.060 g , 1.5 mmol) were mixed in 15 ml distilled water at the room temperature. The mixture was transferred to Parr-Teflon lined stainless steel vessel and was heated at 130 °C for 3 days. After cooling to room temperature, air-stable blue crystals were obtained. Yield: 63% Anal. Calc. for $\text{C}_9\text{H}_{10}\text{NiO}_9$: C, 33.69; H, 3.14. Found: C, 33.31; H, 3.19%. IR (cm^{-1}): 3498-3279 (m, br), 2920(w), 1710(s), 1617(s), 1570(s), 1385(s), 1365(s), 749(m), 743(m).

2.3. Synthesis of $[\text{Ni}(\text{H}_2\text{btc})(\text{OH})(\text{H}_2\text{O})_2]/\text{SiO}_2$ precursor

The catalyst precursor was prepared from mixing an aqueous solution of $[\text{Ni}(\text{H}_2\text{btc})(\text{OH})(\text{H}_2\text{O})_2]$ (3.20 g, 10.0 mmol, 90% Wt) and SiO_2 (0.32 g, 10% Wt), the mixture was stirred and evaporated at 30 °C to dryness.

2.4. Synthesis of silica-supported nickel catalyst, Ni/SiO₂

The nickel- silicon catalyst was obtained through calcinations of $[\text{Ni}(\text{H}_2\text{btc})(\text{OH})(\text{H}_2\text{O})_2]/\text{SiO}_2$ precursor at 700 °C at the atmosphere of static air in the electric furnace and maintaining in this temperature for 6 h.

2.5. Synthesis of $[\text{Ni}(\text{H}_2\text{btc})(\text{OH})(\text{H}_2\text{O})_2]/\text{Al}_2\text{O}_3$ precursor

The catalyst precursor was prepared from mixing an aqueous solution of $[\text{Ni}(\text{H}_2\text{btc})(\text{OH})(\text{H}_2\text{O})_2]$ (3.20 g, 10.0 mmol, 90% Wt) and Al_2O_3 (0.32 g , 10% Wt), the mixture was stirred and evaporated at 30 °C to dryness.

2.6. Synthesis of alumina-supported nickel catalyst, Ni/Al₂O₃

The nickel- alumina catalyst was obtained through calcinations of $[\text{Ni}(\text{H}_2\text{btc})(\text{OH})(\text{H}_2\text{O})_2]/\text{Al}_2\text{O}_3$ precursor at 700 °C at the atmosphere of static air in the electric furnace and maintaining in this temperature for 6 h.

2.7. Preparation of reference catalysts

For comparison, the silica- or alumina- supported Ni reference catalysts were constructed by impregnation method. In first, the support (silica or alumina) was impregnated with an aqueous solution of nickel nitrate. Then, the suspension was stirred for 10 h at 30 °C. The resulting mixture was filtered and the obtained precipitate dried at 120 °C. Finally, the precursor catalyst was calcined at 600 °C for 5 h.

2.8. Sample characterization

Fourier transform infrared (FT-IR) spectra were measured on JASCO 460 spectrophotometer with KBr pellets in the 4000–400 cm^{-1} range. Elemental analyses were performed on Leco, CHNS-932 elemental analyzer. The crystal structure of $[\text{Ni}(\text{H}_2\text{btc})(\text{OH})(\text{H}_2\text{O})_2]$ was obtained via the single-crystal X-ray diffraction technique. Metallic content was determined by ICP in an OPTIMA 2000 DV ICP Optical Emission spectrometer. X-ray diffraction data of the complex was collected on a STOE-IPDS 2T diffractometer using a graphite monochromated Mo $\text{K}\alpha$ radiation ($\lambda=0.71073 \text{ \AA}$). X-ray powder analyses were conducted using a Bruker D8 advance by considering 2θ range from 10° to 70° . The morphology of the catalysts was observed using a MIRA3 TESCAN FE SEM operating at 30 kV. The BET surface areas of the samples were measured by N_2 physisorption using a ASAP 2020 apparatus. Each catalyst sample was degassed under nitrogen atmosphere at 350 °C for 4 h.

2.9. Catalytic activity measurements

Catalytic performance tests for the Fischer-Tropsch reaction were conducted in a fixed bed micro reactor operating at the atmospheric pressure. For each run 0.8 g catalyst was maintained in the reactor by using quartz wool. All catalysts were reduced in situ at the atmospheric pressure in hydrogen/nitrogen mixture (50% vol. H_2) at 400 °C for 8 h before disposal of synthesis gas. Thereafter, the N_2/H_2 was replaced by the current of H_2/CO (2:1). The Fischer-Tropsch reaction was carried out in the range of 280-400 °C. The product stream was analyzed by a GC on a FI detector equipped with a methanizer. The catalytic performance was evaluated in terms two parameters:

$$\text{(I) CO conversion \%} = \{[(\text{Mols of CO}_{\text{in}}) - (\text{Mols of CO}_{\text{out}})] / \text{Mols of CO}_{\text{in}}\} \times 100$$

$$(II) \text{ Selectivity of } j \text{ product } (\%) = \{ \text{Mols of } j \text{ product} / [(\text{Mols of CO}_{in}) - (\text{Mols of CO}_{out})] \} \times 100$$

3. Results and discussion

3.1. Complex characterization

The reaction of $\text{Ni}(\text{NO}_3)_2 \cdot 6\text{H}_2\text{O}$ with 1,3,5-benzenetricarboxylic acid and NaOH in the aqueous solution under the hydrothermal condition led to formation of the air-stable complex $[\text{Ni}(\text{H}_2\text{btc})(\text{OH})(\text{H}_2\text{O})_2]$ **1**. This compound was characterized by elemental analysis, infrared spectroscopy and single crystal X-Ray diffraction.

X-ray crystallographic data determine that complex **1** crystallizes in the monoclinic space group P21/n (Table 1). The asymmetric unit consists of one Ni(II) ion, one H_2btc^- ligand, two coordinated water molecules and one OH^- ion. The title complex is coordination polymer which each metal center is conjoined to two neighboring ones through two μ -oxo bridges. The coordination geometry of Ni(II) ion is a distorted square pyramidal. The Ni(II) ion is coordinated by two oxygen atoms from carboxyl (O3) and carboxylate (O1) groups of H_3btc ligand, three oxygen atoms of two water molecules (O8, O7) and one hydroxyl ion (O9) (Fig.1). Among three functional groups of H_3btc ligand only one carboxyl group is uncoordinated whereas the other carboxyl and carboxylate groups are connected to unidentate coordination mode to Ni(II).

<Place Fig. 1 here>

<Place Table 1 here>

The FT-IR spectrum of **1** (Fig.2) shows the broad band at $3498\text{--}3279\text{ cm}^{-1}$ which is attributed to the anti-symmetric and symmetric stretching vibrations of coordinated water molecules. The band appearing around 1710 cm^{-1} is assigned to $\nu(\text{C=O})$ of the carboxyl groups and is confirmed that carboxyl groups are not fully deprotonated. The intense band at 1617 cm^{-1} indicates that the carboxyl group is deprotonated. The bands observed at 1246 and 1244 cm^{-1} are ascribed to $\nu(\text{C-O})$ vibrations. In the desired complex, the presence of carboxylate group is reflected by IR spectrum in bands of the anti-symmetric, $\nu_a(\text{COO})$, and symmetric, $\nu_s(\text{COO})$, stretching vibrations at 1570 and 1385 cm^{-1} , respectively. The frequency difference between anti-symmetric and symmetric stretching vibrations of the of the carboxylate group is $\Delta\nu = 185$ which is suggested monodentate coordination mode of the carboxylate group to the Ni(II) ion. The C-H stretching vibrations of the

benzene ring of H₃Btc ligand emerge at 3105 and 3070 cm⁻¹ [26]. The two C–H in-plane bending modes observe at 1187 and 1181 cm⁻¹. The band at 890 cm⁻¹ can be assigned to C–H out-of-plane bending mode [27, 28].

<Place Fig. 2 here>

3.2. Catalysts characterization

The FT-IR spectra of both catalysts prepared by thermal decomposition of inorganic precursor complex are shown in Fig.3. In the IR spectrum of Ni/SiO₂, the broad bonds at 3420 cm⁻¹ is assigned to OH stretching vibration of physically adsorbed water and the H–OH bending vibration is appeared at 1625 cm⁻¹. The intensive band at 1107 cm⁻¹ is assigned to Si–O–Si anti-symmetric stretching vibration and the band observed at 804 cm⁻¹ are imputed to the symmetric stretching vibration of the Si–O–Si. The OSi–O bending vibration emerges at 535 cm⁻¹. The band at 594 cm⁻¹ is attributed to Si–O bending mode [29–31]. Investigating of the FT–IR spectrum of alumina-supported nickel catalyst show that the bands centered at 3427 cm⁻¹ and 1644 cm⁻¹ are belonged to OH stretching vibration and H–OH bending mode of physically adsorbed water, respectively. The peak corresponding to 1154 cm⁻¹ is assigned to Al–O–Al anti-symmetric bending mode. The vibration bands at 850, 676 and 533 cm⁻¹ are attributable to bending and stretching modes of AlO₆ [32].

<Place Fig. 3 here>

The composition of the synthesized and reference catalysts determined by ICP analysis. The loading of Ni in the catalysts prepared by thermal decomposition of inorganic precursor supported on silica and alumina are 60.2 and 58.6, respectively. The loading of Ni in the reference catalysts are 52.4 % and 51.9 % for supporting silica and alumina, respectively.

Characterization of Ni catalysts prepared by thermal decomposition of inorganic precursors were carried out by using X-ray diffraction, and the obtained X-ray diffractograms of the silica- and alumina- supported Ni catalysts are depicted in Fig. 4. The XRD pattern of the nickel- silica calcined catalyst synthesized from inorganic precursor contains diffraction peaks at $2\theta = 38.7, 48.7, 58.6, 69.1^\circ$, which are assigned to diffraction of NiO₂. Characteristic peaks of SiO₂ at $2\theta = 25.9, 35.6$ are observed for calcined catalyst. The nickel- alumina synthesized catalysts displays

the characteristic XRD peaks of NiO_2 at $2\theta = 38.7, 48.7, 58.6, 69.1^\circ$. The diffraction peaks at $2\theta = 35.3, 46.4$ are attributed to Al_2O_3 . The diffractograms of reference catalysts prepared by impregnation include diffraction peaks at $2\theta = 37.2, 43.2, 62.8^\circ$, which are allocated to NiO phase (Fig. 5). Comparison of the X-ray diffraction peaks broadening in the synthesized catalysts and the reference samples display that crystallite size is smaller for the constructed catalysts. The average particle sizes were determined by Scherrer's equation. The average crystallite sizes of synthesized catalysts supported on SiO_2 and Al_2O_3 are 58.1 and 54.3 nm, respectively, while the average sizes of reference catalysts are 84.6 and 73.5 nm for silica and alumina supported, respectively. These results show that the fabricated catalysts lead to the improvement of the scattering of the metal and simplify producing smaller particles than the reference catalysts.

<Place Fig. 4 here>

<Place Fig. 5 here>

The morphological properties of the catalysts were determined using scanning electron microscopy (SEM). The SEM micrographs of the catalysts prepared by thermal decomposition of inorganic precursors and impregnation method are displayed in Fig. 6 and Fig. 7, respectively. The morphological features of the synthesized catalysts and reference catalysts are different. The electron micrographs obtained from Ni/SiO_2 and $\text{Ni/Al}_2\text{O}_3$ catalysts synthesized through inorganic precursor path have smaller particles in comparison with Ni/SiO_2 and $\text{Ni/Al}_2\text{O}_3$ reference catalysts. Moreover, the grade of agglomeration fabricated catalysts is lower than reference catalysts which are shown that preparing catalysts via inorganic precursor is more appropriate route toward impregnation method.

<Place Fig. 6 here>

<Place Fig. 7 here>

The BET results of the catalysts constructed by thermal decomposition of inorganic precursors and the reference catalysts created by impregnation are presented in Table 2. As observed from Table 2, both synthesized catalysts have higher surface area than the reference catalysts. The usage of the acceptable procurement procedure (thermal decomposition of inorganic precursor complex) lead to enhancement in the specific surface areas of the these catalysts, which is a persuasive evidence for

the improvement in the dispersion of the active oxide phase and the increment in catalytic performance of these synthesized catalysts.

<Place Table 2 here>

3.3. Catalytic performance

The catalytic performance of the fabricated and reference catalysts were evaluated at atmospheric pressure in the temperature range 280-400 °C with H₂/CO ratio of 2.

Generally, an increment in the reaction temperature leads to an increasing in the catalytic activity, moreover, it has been obvious that the reaction temperature should not be too low [33]. The CO conversion is negligible at low reaction temperature which is afforded to low catalytic performance. The enhancing temperature promotes CO dissociation, and provides more surface C atoms for forming hydrocarbons. On the other hand, with raising reaction temperature, methane formation increases due to the abundant surface H atoms [34]. Apart from the reaction temperature, the preparation method of catalyst remarkably affects the CO conversion and hydrocarbon selectivity. As observed from Fig. 8, the CO conversion percentages of Ni catalysts prepared by thermal decomposition of inorganic precursor and impregnation have increased with increment temperature from 280 °C to 400 °C. The CO conversion is higher for Ni-SiO₂ and -Al₂O₃ catalysts synthesized through inorganic precursor approach compared to reference catalysts produced from impregnation method in all studied temperature. The catalytic activity of calcined catalysts was obtained by different procedures increased with enhancing temperature from 280 to 400 °C (Fig. 9). According to obtained results, the constructed Ni-Al₂O₃ catalyst has higher selectivity to light olefins products and lower methane selectivity than the Ni-SiO₂ catalyst. On the other side, both of the reference catalysts have lower selectivity to light olefins products and higher methane selectivity compared to the synthesized catalysts. It can be seen that, for Ni-SiO₂ sample, the optimal operating temperature equals 340 °C given the high selectivity of light olefins products and low methane selectivity whereas for the Ni-Al₂O₃ sample the optimal temperature is 360 °C.

In general, the fabricated Ni catalysts have premier catalytic performance in comparison with the findings achieved for the reference Ni-catalysts prepared by impregnation method. These results

due to the synthetic route used for the synthesized Ni catalyst allows it having high BET specific surface area, small particle size, low degree agglomeration and good active phase dispersion.

Conclusion

The thermolysis of $[\text{Ni}(\text{H}_2\text{btc})(\text{OH})(\text{H}_2\text{O})_2]/\text{SiO}_2$ and $[\text{Ni}(\text{H}_2\text{btc})(\text{OH})(\text{H}_2\text{O})_2]/\text{Al}_2\text{O}_3$ as inorganic precursors was used for construction of Ni/ SiO_2 and Ni/ Al_2O_3 catalyst. The reference catalysts were prepared through impregnation method. The SEM micrographs of samples display that synthesized catalysts have lower particle sizes and agglomeration in comparison with reference catalysts. These results are in good agreement with the BET outcomes; it means that the catalysts prepared by thermal decomposition of inorganic precursors have higher surface area than reference catalysts. Activity of the catalysts in FTS was investigated at 280–400 °C with H_2/CO ratio of 2 and specified that the fabricated catalysts are more active than impregnation reference samples. Furthermore, it can be concluded that preparing catalysts by inorganic precursor is more suitable procedure toward impregnation method.

Acknowledgements

The financial support from the Iranian National Science Foundation (Grant No. 95834583) is gratefully acknowledged.

Reference

- [1] Y. Traa, Chem. Commun. 46 (2010) 2175–2187.
- [2] M. Höök, K. Aleklett, Int. J. Energy Res. 34 (2010) 848–864.
- [3] M. Arsalanfar, A.A. Mirzaei, H. Atashi, H.R. Bozorgzadeh, S. Vahid, A. Zare, Fuel Process. Technol. 96 (2012) 150–159.
- [4] M.E. Dry, Catal. Today 71(2002) 227–241.
- [5] A.R. de la Osa, A. De Lucas, A. Romero, J.L. Valverde, P. Sánchez, Fuel 90 (2011) 1935–1945.
- [6] A. Zare, A. Zare, M. Shiva, A.A. Mirzaei, J. Ind. Eng. Chem. 19 (2013) 1858–1968.

- [7] A.A. Mirzaei, M.K. Rouhoullah, H. Atashi, M. Arsalanfar, S. Shahriari, J. Ind. Eng. Chem. 18 (2012) 1242–1251.
- [8] V.A. de la Peña O'Shea, M.C. Alvarez-Galvan, J.M. Campos-Martin, J.L.G. Fierro, Catal. Lett. 100 (2005) 105–116.
- [9] B.H. Davis, Catal. Today 84 (2003) 83–98.
- [10] M. Ding, Y. Yang, J. Xu, Z. Tao, H. Wang, H. Wang, H. Xiang, Y. Li, Appl. Catal., A 345 (2008) 176–184.
- [11] A.A. Mirzaei, B. Shirzadi, H. Atashi, M. Mansouri, J. Ind. Eng. Chem. 18 (2012) 1515–1521.
- [12] J. Loosdrecht, A.M. Kraan, A.J. Dillen, J.W. Geus, Catal. Lett. 41 (1996) 27–34.
- [13] H. Arai, K. Mitsuishi, T. Seiyama, Chem. Lett. 13 (1984) 1291–1294.
- [14] B.C. Enger, A. Holmen, Cat. Rev. - Sci. Eng. 54 (2012) 437–488.
- [15] M.A. Vannice, R.L. Garten, J. Catal. 56 (1979) 236–248.
- [16] C.H. Bartholomew, R.B. Pannell, J.L. Butler, J. Catal. 65 (1980) 335–347.
- [17] G.A. Hadjigeorgiou, J.T. Richardson, Appl. Catal. 21 (1986) 11–35.
- [18] G.A. Hadjigeorgiou, J.T. Richardson, Appl. Catal. 21 (1986) 47–59.
- [19] B. Ernst, S. Libs, P. Chaumette, A. Kiennemann, Appl. Catal., A 186 (1999) 145–168.
- [20] M. Feyzi, A.A. Mirzaei, J Fuel Chem Technol 40 (2012) 1435–1443.
- [21] A. Miroliaee, A.R. Salehirad, A.R. Rezvani, Mater. Chem. Phys. 151 (2015) 312–317.
- [22] C.-D. Wu, A.-G. Hu, L. Zhang, W.-B. Lin, J. Am. Chem. Soc. 127 (2005) 8940–8941.
- [23] L. Ma, C. Abney, W. Lin, Chem. Soc. Rev. 38 (2009) 1248–1256.
- [24] T. Uemura, N. Yanai, S. Kitagawa, Chem. Soc. Rev. 38 (2009) 1228–1236.

- [25] S. Saheli, A.R. Rezvani, J. Mol. Struct. 1127 (2017) 583–589.
- [26] G. Socrates, *Infrared Characteristic Group of Frequencies*, Wiley, New York, 1980.
- [27] G. Varasanyi, *Assignments of Vibrational Spectra of Seven Hundred Benzene Derivatives*, Wiley, New York, 1974.
- [28] K. Akhbari, A. Morsali, J. Iran. Chem. Soc. 5 (2008) 48–56.
- [29] E.M. Fixman, M.C. Abello, O. F. Gorriz , L.A. Arrúa, Appl. Catal., 319 (2007) 111–118.
- [30] M.A. Ermakova, D.Yu. Ermakov, Catal. Today 77 (2002) 225–235.
- [31] V.A. Dzis'ko, S.P. Noskova, L.G. Karachiev, M.S. Borisova, V.G. Bolgova, T.Ya. Tyulikova, Sov Appl Mech 5 (1969) 327–333.
- [32] M.-G. Ma, J.-F. Zhu, Mater. Lett. 63 (2009) 881–883.
- [33] M. Feyzi, A.A. Mirzaei, H.R. Bozorgzadeh, J. Natural Gas Chem. 19 (2010) 341–353.
- [34] L. Tian, C.F. Huo, D.B. Cao, Y. Yang, J. Xu, B.S. Wu, H.W. Xiang, Y.Y. Xu, Y.W. Li, J MOL STRUC THEOCHEM, 941 (2010) 30–35.

Table 1Crystallography data for [Ni(H₂btc)(OH)(H₂O)₂].

Complex	1
Empirical formula	C ₉ H ₁₀ NiO ₉
Formula Weight	320.86
Crystal system	Monoclinic
Space group	P21/n
Crystal size (mm)	0.09 × 0.09 × 0.40
<i>a</i> [Å]	6.8658(14)
<i>b</i> [Å]	18.849(4)
<i>c</i> [Å]	8.5608(17)
β [°]	92.98(3)
Volume/Å ³	1106.4(4)
Temperature [K]	293(2)
Z	4
D _{calcd} ·[g cm ⁻³]	1.926
F(000)	656
Reflections collected /unique	4287/1937
wR ₂	0.0920
R	0.0429

Table 2

BET results of synthesized and reference catalysts.

synthesized Sample	BET surface area (m ² /g)	reference Sample	BET surface area (m ² /g)
Ni/SiO ₂	98	Ni/SiO ₂	30
Ni/Al ₂ O ₃	110	Ni/Al ₂ O ₃	45

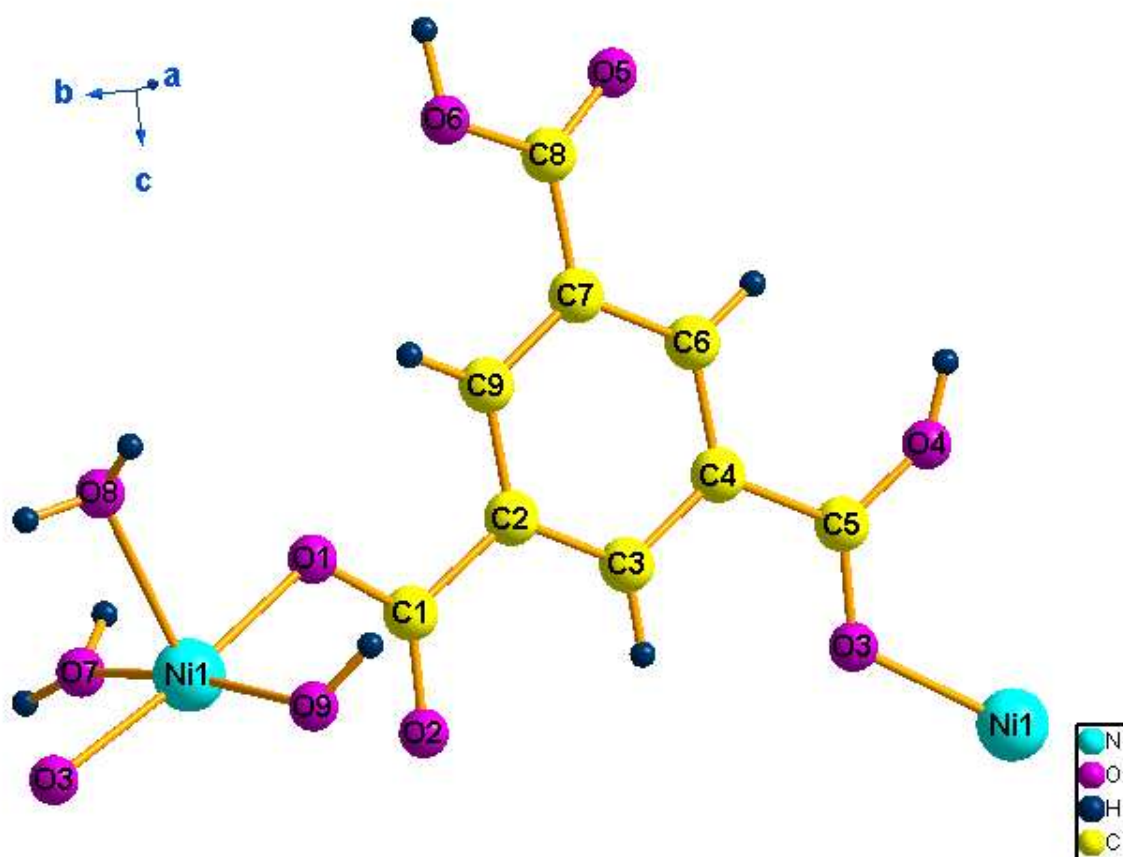


Fig.1. The coordination environment of Ni(II) ion in complex 1.

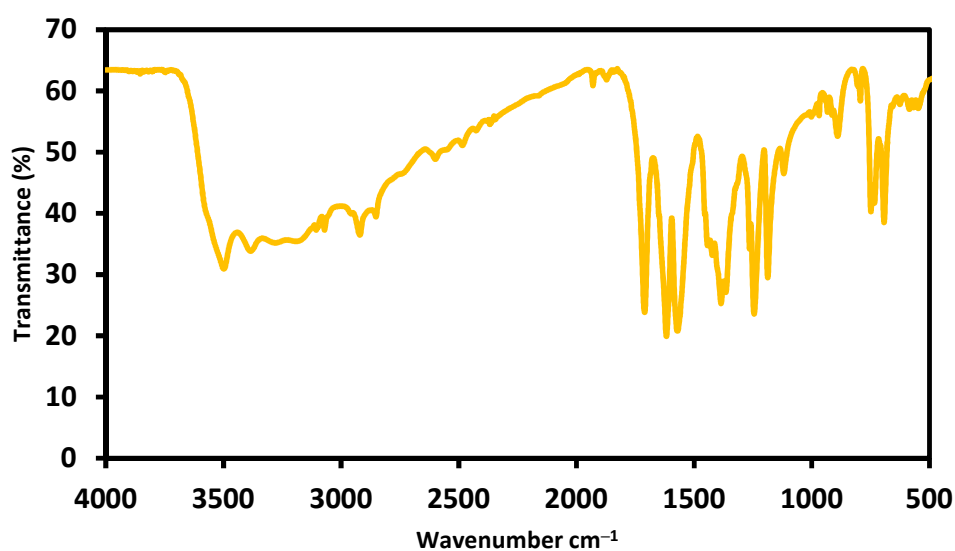


Fig. 2. The FT-IR spectrum of complex 1 prepared under hydrothermal condition.

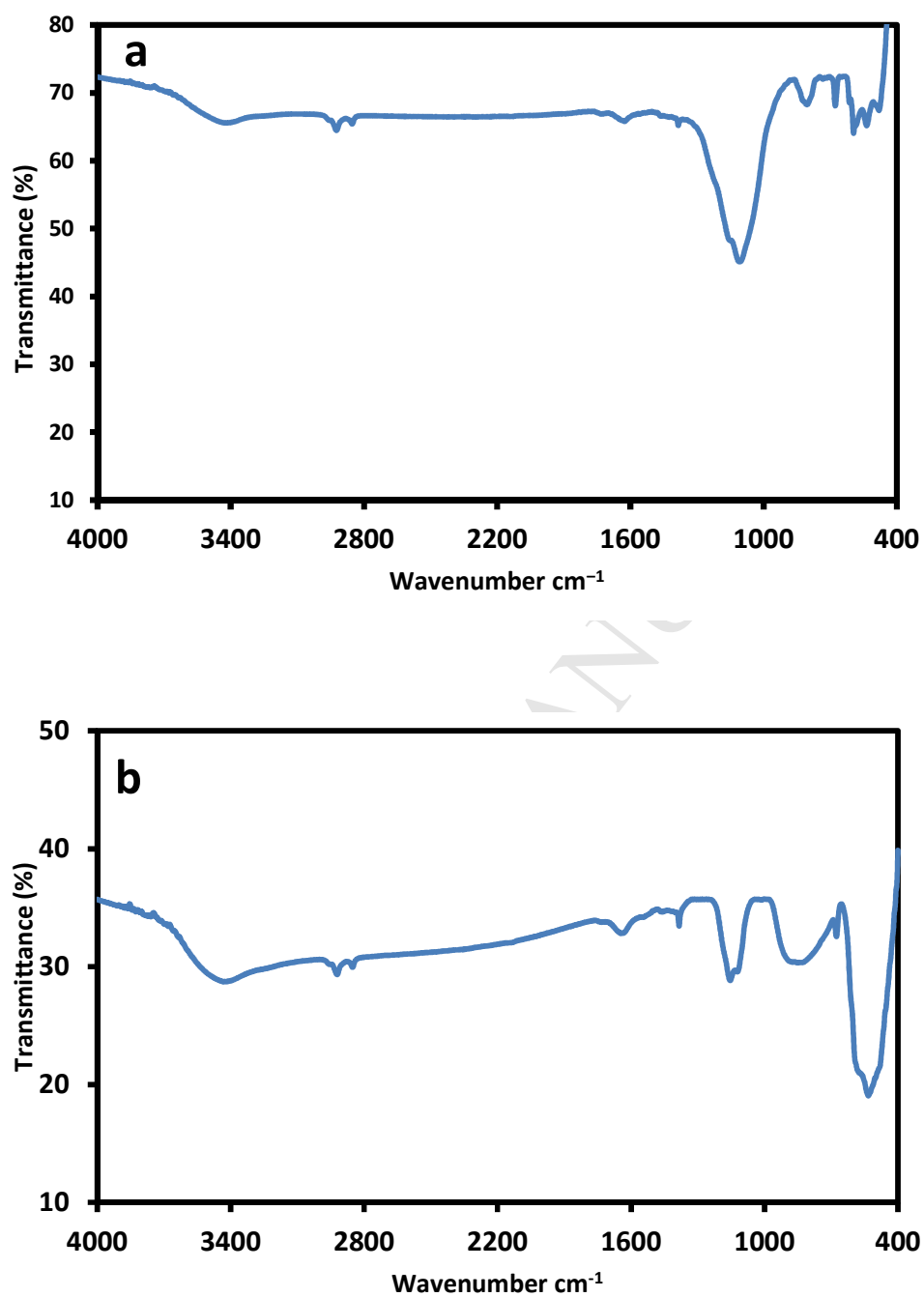


Fig. 3. The FT-IR spectra of synthesized Ni catalysts supported on SiO_2 (Fig.3a.) and Al_2O_3 (Fig. 3b.).

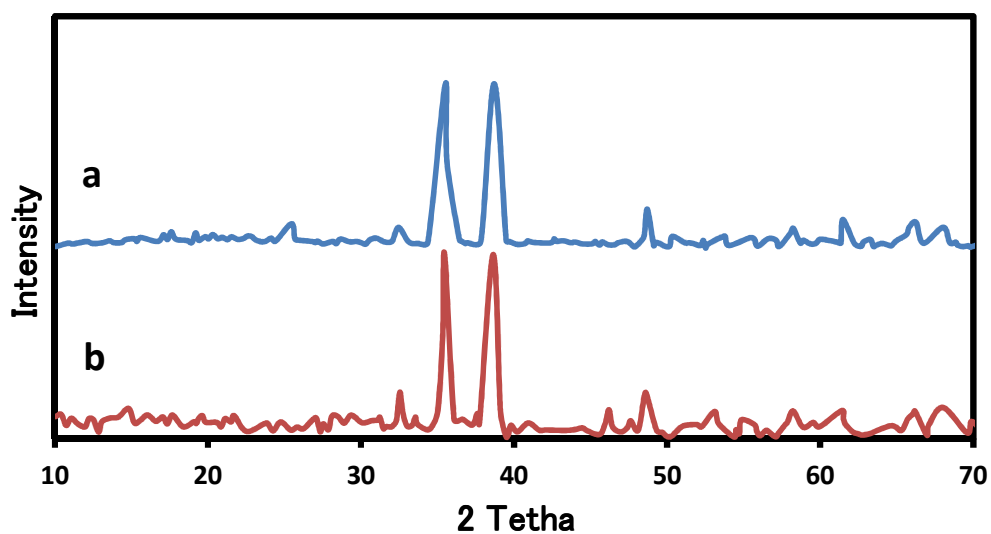


Fig. 4. The XRD patterns of Ni /SiO₂ (Fig.4a.) and Ni /Al₂O₃ (Fig. 4b.) synthesized catalysts prepared by thermal decomposition of inorganic precursor.

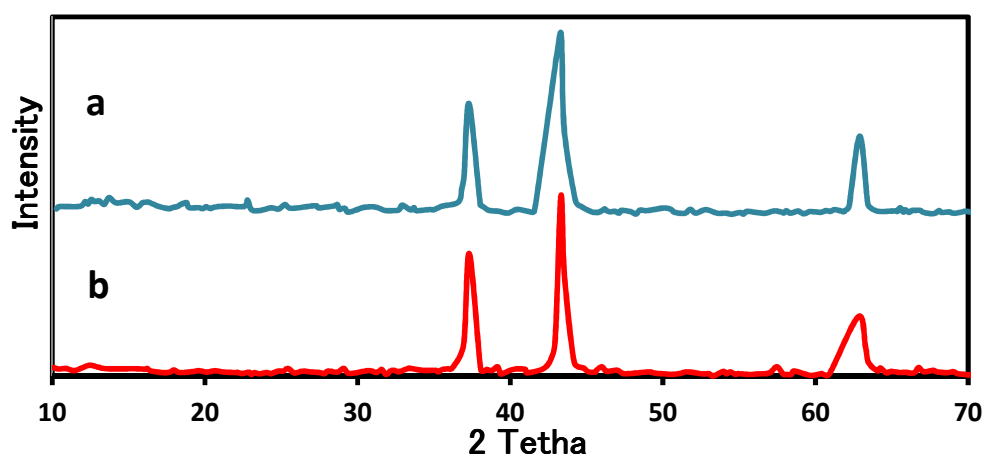


Fig. 5. The XRD patterns of Ni /SiO₂ (Fig.5a.) and Ni /Al₂O₃ (Fig. 5b.) reference catalysts prepared by impregnation method.

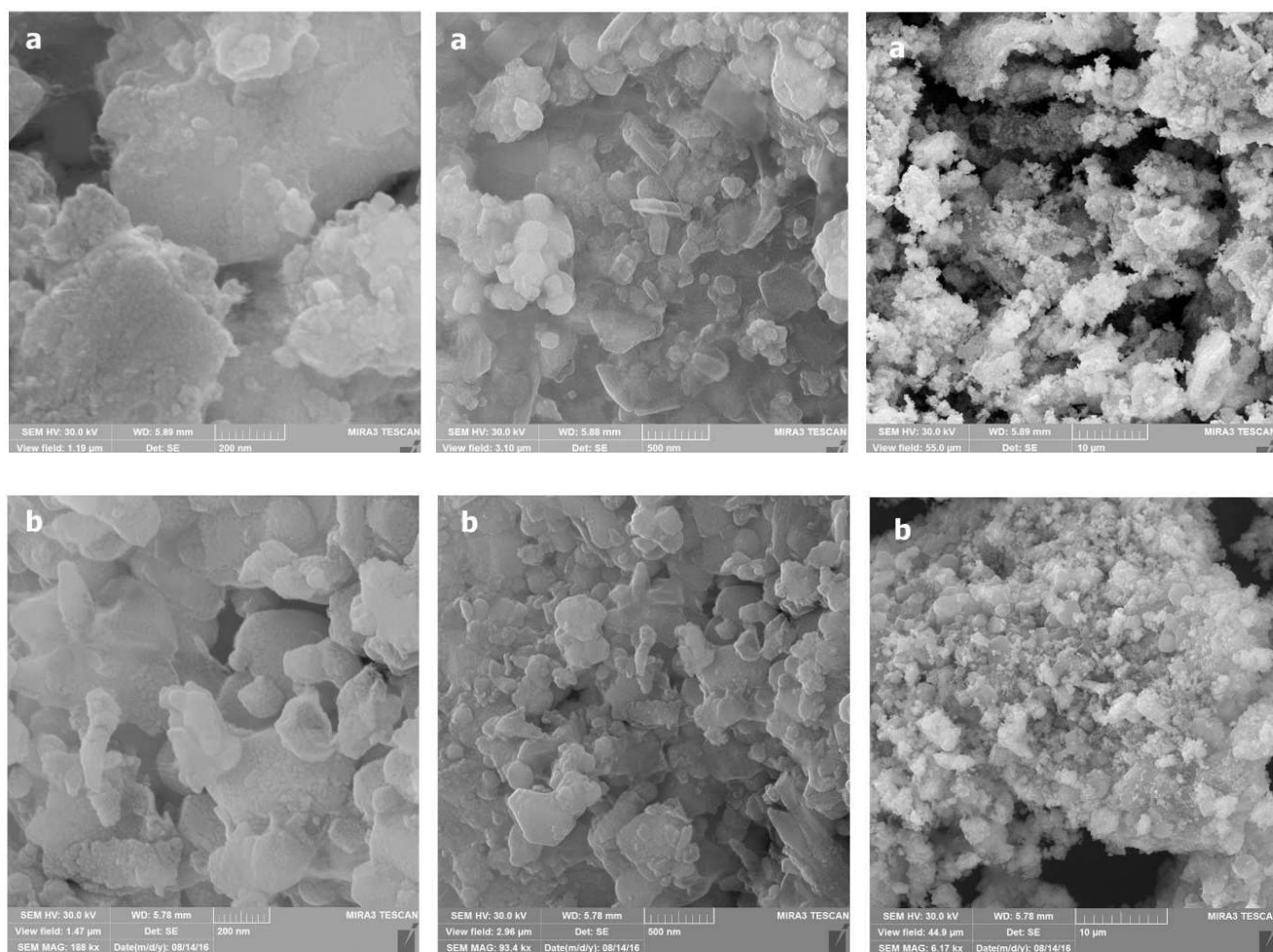
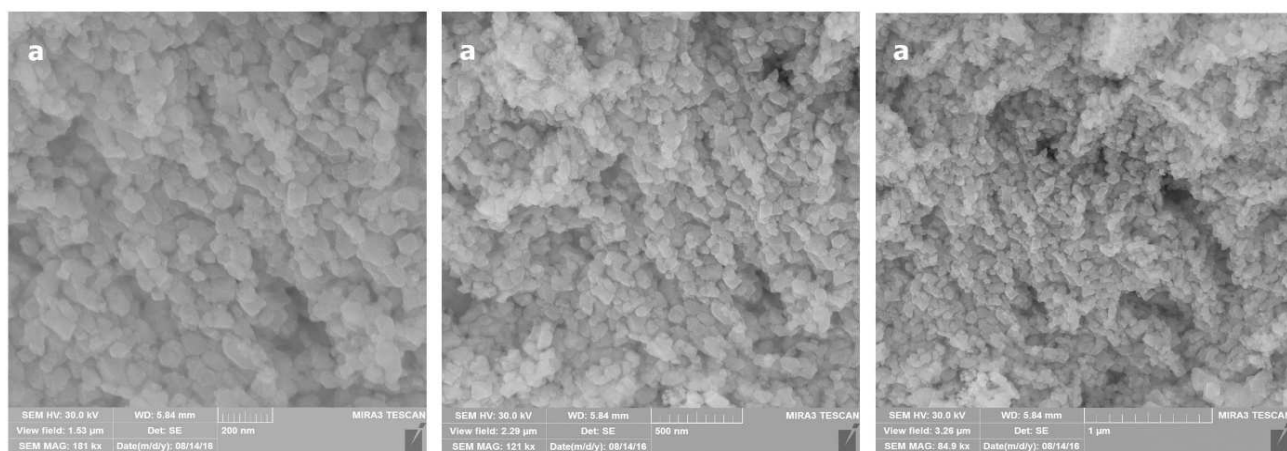


Fig. 6. SEM micrographs of synthesized catalysts a) Ni/SiO_2 and b) $\text{Ni}/\text{Al}_2\text{O}_3$.



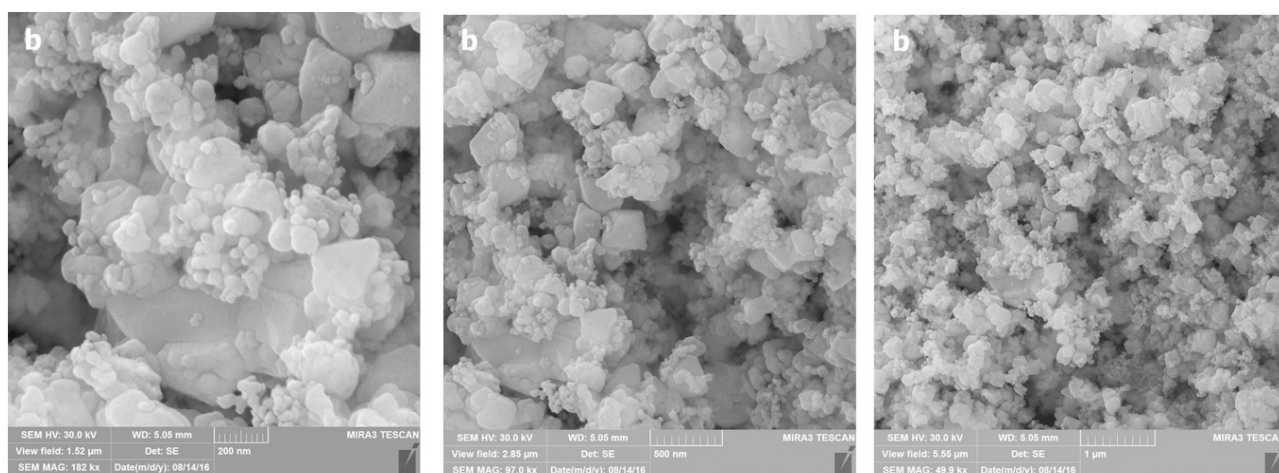


Fig.7. SEM micrographs of reference catalysts a) Ni /SiO₂ and b) Ni /Al₂O₃.

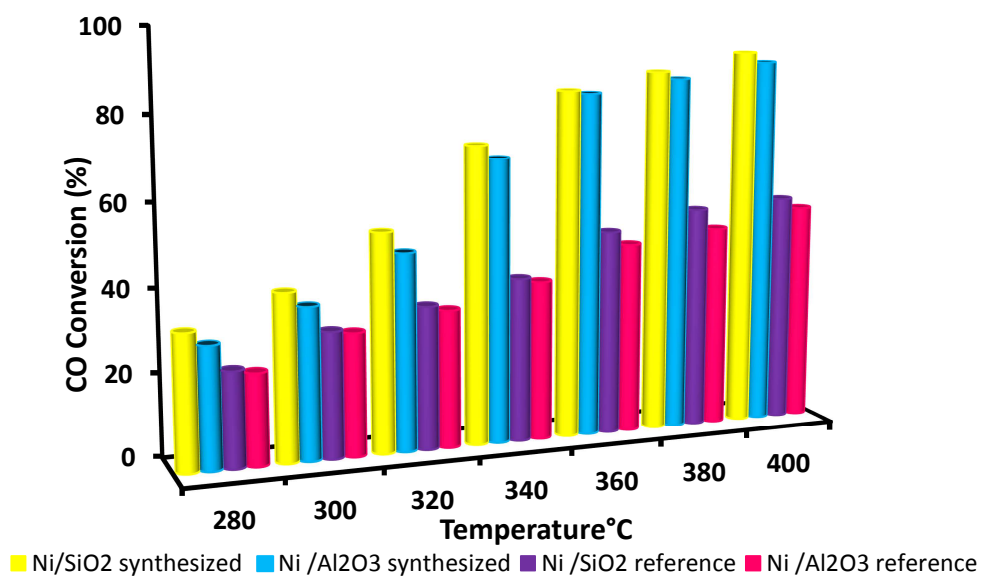
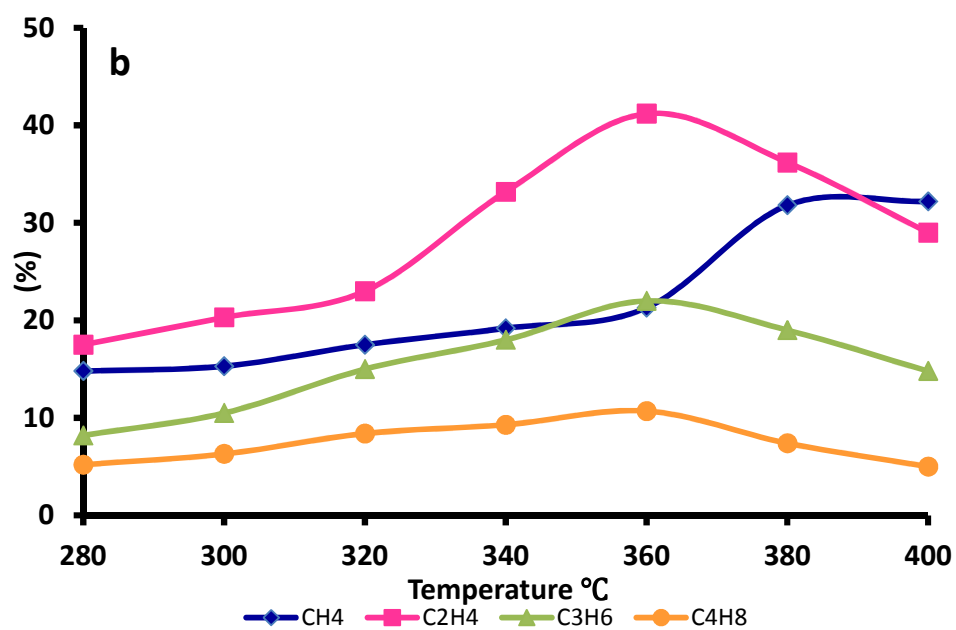
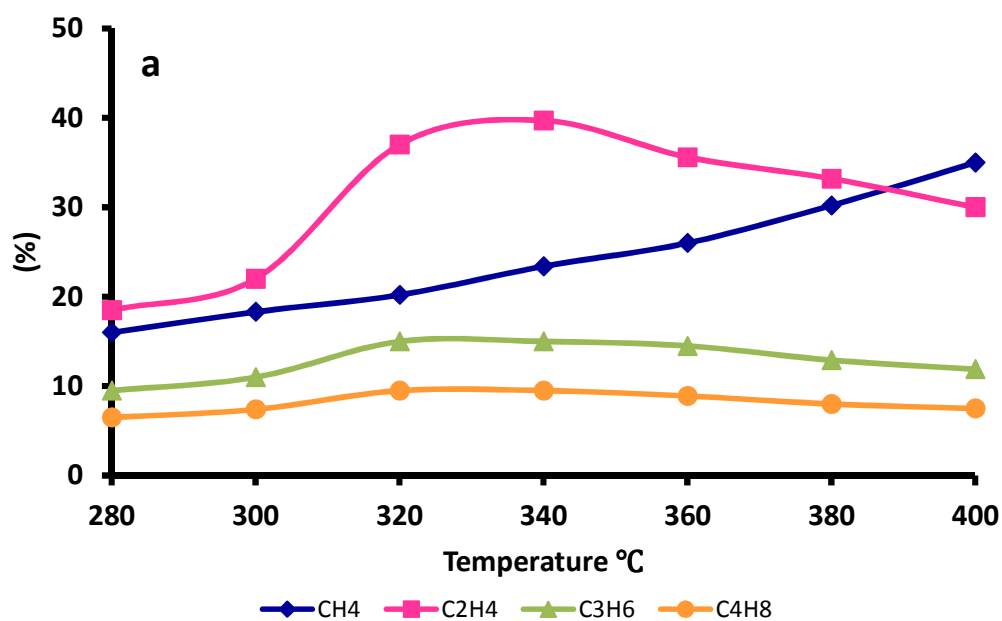


Fig. 8. Effect of reaction temperature on CO conversion percentages of synthesized and reference catalysts.



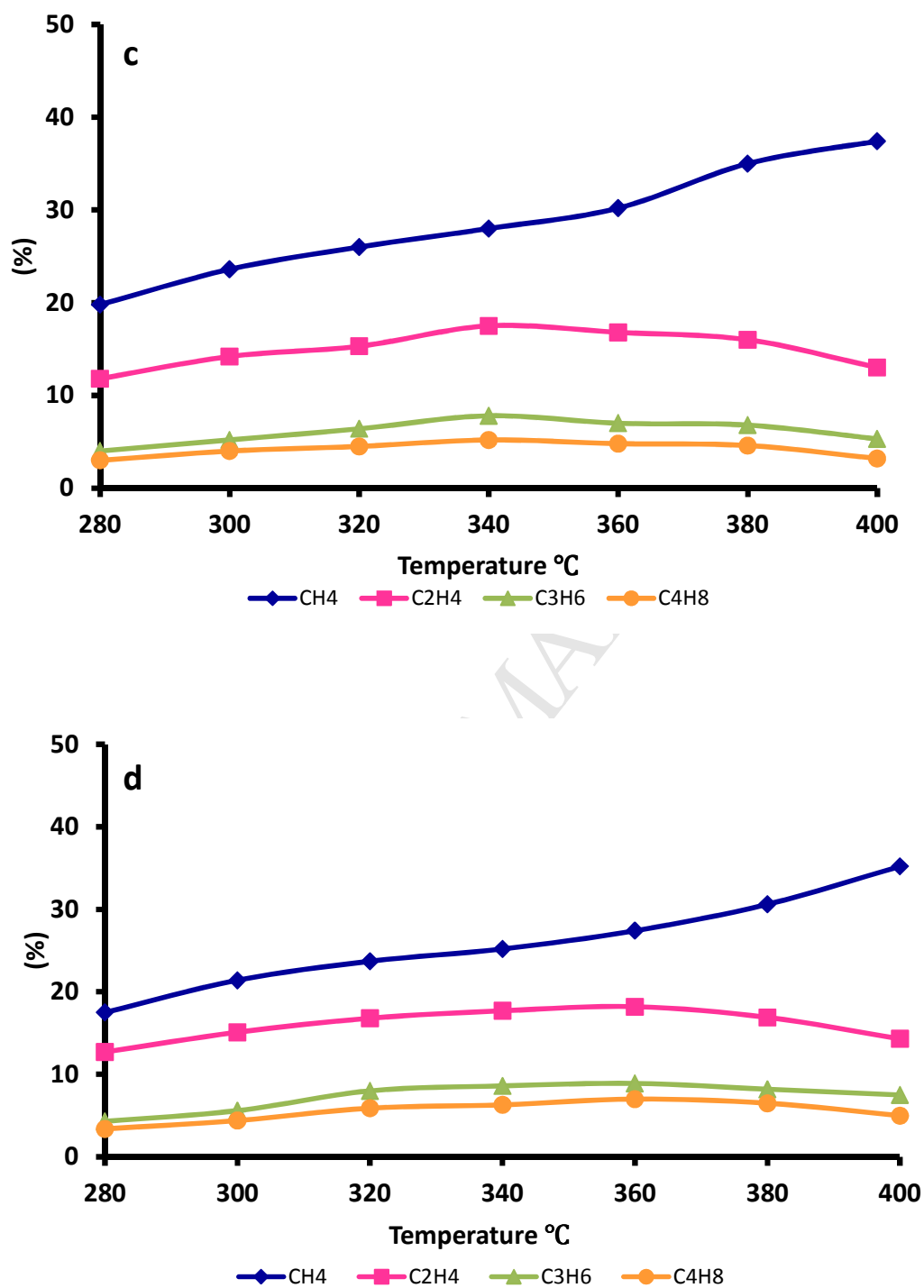


Fig. 9. Effect of different reaction temperatures on the catalytic performance of synthesized (a: Ni /SiO₂, b: Ni /Al₂O₃) and reference(c: Ni /SiO₂, d: Ni /Al₂O₃) catalysts.

Highlights

- The fabricated catalysts are more active than impregnation reference samples.
- The Ni catalysts were synthesized through new inorganic precursor.
- The synthesized catalysts have higher selectivity to light olefins than reference conventional samples.